IMPACT OF THE G PROTEIN-COUPLED ESTROGEN RECEPTOR ON ENDOTHELIAL DERIVED ARTERIAL STIFFENING

AN HONORS THESIS

SUBMITTED ON THE TWENTY-SECOND DAY OF APRIL, 2021 TO THE DEPARTMENT OF BIOMEDICAL ENGINEERING

IN PARTIAL FULFILLMENT OF THE REQUIREMENTS OF THE HONORS PROGRAM OF NEWCOMB TULANE COLLEGE

TULANE UNIVERSITY

FOR THE DEGREE OF

BACHELOR OF SCIENCES IN ENGINEERING

WITH HONORS IN BIOMEDICAL ENGINEERING

BY

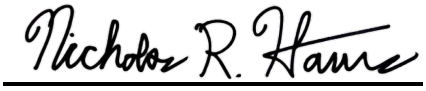

Nicholas Harris

APPROVED:

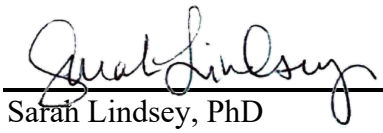

Sarah Lindsey, PhD
Director of Thesis

Kristin Miller, PhD
Second Reader

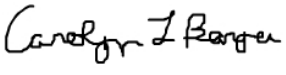

Carolyn Bayer, PhD
Third Reader

ABSTRACT

Nicholas Harris. Impact of the G Protein-Coupled Estrogen Receptor on Endothelial Derived Arterial Stiffening.

(Sarah Lindsey, PhD, Department of Pharmacology, Tulane University School of Medicine)

Cardiovascular disease is the leading cause of death for men and women in the United States. Arterial stiffness is an early indicator of hypertension that is associated with a change in the extracellular matrix composition leading to a decrease in vessel elasticity and increased cardiac afterload. In endothelial cells, the G protein-coupled estrogen receptor (GPER) activates endothelial nitric oxide synthase to counteract vasoconstriction and vascular remodeling. However, the interaction between endothelial GPER and arterial stiffening remains unknown. Here, we investigated the impact of chronic nitric oxide deficiency on pulse wave velocity, an *in vivo* measurement of arterial stiffness, vascular structure, and the role of GPER. A cohort composed of male wild-type and GPER knockout mice were chronically treated with a nitric oxide synthase inhibitor, N_{ω}-Nitro-L-arginine methyl ester hydrochloride (L-NAME), for three weeks. Pre- and post-treatment blood pressures were collected via tail-cuff plethysmography, ultrasound imaging was used to monitor pulse wave velocity, and pressure myography of the mesenteric artery *ex vivo* was used to assess vessel reactivity and structure.

We found no change in blood pressure or mesenteric wall thickness over the course of L-NAME treatment. Pulse wave velocity significantly increased in response to L-NAME in wild-type mice but not in GPER knockout mice. Both L-NAME treatment and genetic deletion of GPER significantly increased myogenic tone. Interestingly, L-NAME treatment in GPER knockout mice reduced rather than exacerbated the myogenic response. These results provide evidence of the complicated role of GPER and nitric oxide in endothelial-mediated responses.

Further testing is needed to understand estrogen's effect on endothelial dysfunction; the results of which could reveal important therapeutic targets.

ACKNOWLEDGEMENTS

I would like to thank Dr. Lindsey for her support and guidance through this project and my other endeavors. Also, I would like to thank the other members of the Lindsey Lab, Ben Ogola, Bruna Visniauskas, Isabella Kilanowski-Doroh, Gabby Clark-Patterson, Zaidmara Diaz, Murad Laradji, and Alec Horton, for their continued support. Thank you to Dr. Miller and Dr. Bayer, Tulane Biomedical Engineering, for their continued academic guidance. Likewise, I would like to thank Tulane's Department of Biomedical Engineering for giving me the tools to grow professionally both in research and beyond. Finally, I would like to thank my family: my mom for her loving support throughout my life, my brother for giving me the strength to chase my dreams, and my grandparents, who I am grateful to have celebrate my successes and console me in my lows.

TABLE OF CONTENTS

Table of Figures

1. Introduction

Cardiovascular disease (CVD) is the leading cause of death for men and women in the United States [1]. Hypertensive cardiovascular disease can be detected early by measuring the stiffness of the arteries. Arterial stiffening is associated with a change in the extracellular matrix composition leading to a decrease in vessel elasticity, increased cardiac afterload, and end-organ damage [2-4]. Although men are more at risk for CVD, post-menopausal women exhibit a similar or greater risk of developing CVD. This greater risk is attributed to a drop of endogenous estrogen in women after menopause. The G protein-coupled estrogen receptor (GPER) is present in both vascular smooth muscle and endothelial cells [5]. In endothelial cells, GPER contributes to nitric oxide (NO) production [6], leading to vasodilation of the artery. Furthermore, endothelial GPER activation has not yet been linked to arterial stiffening. For this study, the effects of chronic NO deficiency on pulse wave velocity, vascular reactivity, and vascular structure will be determined. Additionally, endothelial GPER's role in vascular stiffening and remodeling will be assessed. We hypothesize chronic endothelial NO synthase (eNOS) inhibition or genetic deletion of GPER will result in arterial stiffening, leading to increased pulse wave velocity, decreased vessel reactivity, and increased vascular thickness.

The study consisted of four different mice cohorts. Two of the groups were male wild-type mice; one group was a control while the other received treatment. Furthermore, the other two groups were GPER global knockout mice where one group was a control, and one received treatment. To chronically inhibit eNOS, the treatment groups received N_{ω}-Nitro-L-arginine methyl ester hydrochloride (L-NAME) in the drinking water for three weeks. To monitor the effectiveness of L-NAME to induce arterial stiffening, blood pressure and pulse wave velocity were monitored pre- and post-treatment [7, 8]. Vessel reactivity and structure were assessed using active and passive pressure myography of the second-order mesenteric artery [9]. Active pressure myography tested vessel reactivity through myogenic tone, or the endothelium-independent constriction of the vessel, whereas passive pressure myography tested vessel structure. Vascular

remodeling is an important aspect of arterial stiffening as when the structure of the artery changes, the function also changes. The results of this study, along with data collected on vascular smooth muscle cell stiffening, opens new avenues for targeting the endothelium and GPER to counteract cardiovascular disease.

2. Background

2.1 Sexual Dimorphism in Cardiovascular Physiology

Although cardiovascular disease is the leading cause of death for both men and women in the United States, men are at a significantly larger risk of dying of cardiovascular disease than women [10] until menopause. After menopause, the gap in cardiovascular mortality between the sexes closes [11]. This increased risk in females is attributed to a decrease in endogenous estrogen in females during and after menopause [12]. Observational studies following postmenopausal women have shown that hormonal replacement therapy reduces the risk for coronary heart disease when started at the beginning of menopause [13]. That being said, hormone replacement therapy does not lower the risk of heart disease to premenopausal values [14]. The reasoning behind the discrepancy of estrogen's protective effects in aging women versus premenopausal women is still unknown.

2.2 Estrogen Receptors

2.2.1 Nuclear Estrogen Receptors

Endogenous estrogen is normally found in three forms in the body: estrone (E1), estradiol (E2), and estriol (E3). This paper will focus on estradiol, as it is the most potent estrogen receptor agonist. Mainly produced in the follicles in the ovaries in women, and, to a smaller extent, the testes in men, the estrogen is released into the blood stream. As a steroid hormone, estrogen diffuses into any cell within the body due to its ability to cross the plasma membrane. Once inside a cell, estrogen binds to the estrogen receptors, ER-α and ER-β, that form a homo- or heterodimer with the other ER once estrogen is bound [15]. The dimer then crosses the nuclear membrane and binds to estrogen response elements that allow for transcription of specific genes. Due to the initiation of transcription, activation of nuclear ER leads to long-term effects that can last hours or even days.

2.2.2 G Protein-Coupled Estrogen Receptor

In addition to the nuclear estrogen receptors, a membrane-bound estrogen receptor, GPR30 or G protein-coupled estrogen receptor (GPER), binds to estrogens to produce more immediate cellular effects. GPER is found throughout the body in multiple organs including the brain, heart, kidneys, arteries, and pancreas [16]. In the cell, GPER is localized to both the plasma membrane and the endoplasmic reticulum [17]. Agonists of GPER include E2, which binds to all ERs, and G-1, which only binds to GPER. Once activated, GPER signals the release of other signaling molecules such as cyclic AMP, calcium, inositol triphosphate, as well as activating the ERK/MAPK pathway [18-20]. GPER plays many roles throughout the body including metabolism, nervous system activity, regulation in reproductive tissues, and cardiovascular regulation. GPER's role in cardiovascular health will be further explored later.

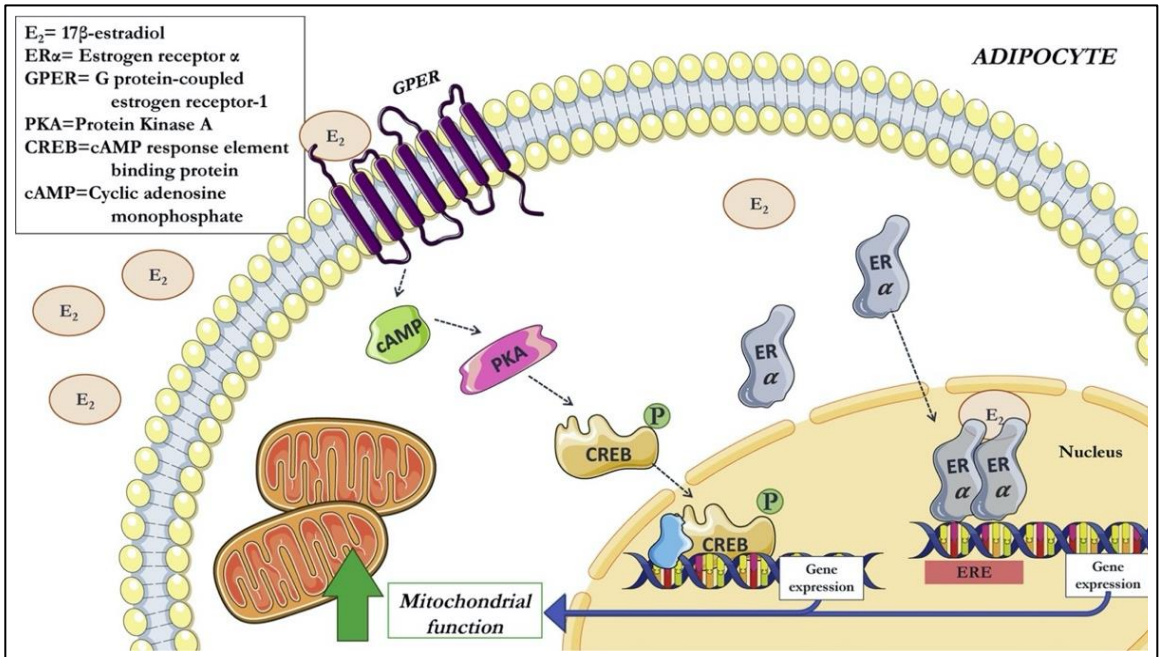

Figure 1. Overview of nuclear ER and GPER pathways [21].

2.3 Small Vessel Mechanics

2.3.1 Young's Modulus

The material properties of the elastic and collagen fibers determine the mechanical behavior of the artery during times of deformation, or strain, due to applied stress. This relationship between stress and strain for any material can be represented as a ratio and is called the elastic, or Young's, modulus. The differing arrangement of fibers along the axial and circumferential directions cause the artery to behave anisotropically, different Young's moduli for the axial and circumferential directions [21]. For small vessels, Young's modulus is most important in the circumferential direction as a change in arterial pressure will cause a change in diameter, and small vessels are tethered to connective tissue, restricting their movement axially.

2.3.2 Myogenic Tone

An important property of small arteries is the ability to maintain constant blood pressure without outside stimulation, called myogenic tone. This mechanism is especially important in small vessels that can be easily damaged under high pressures. By constricting under high pressures, the vessel maintains a constant flow, thus maintaining the delivery of blood to downstream organs. Maintaining a constant flow in small resistance arteries is imperative as rapidly changing pressure is dangerous due to altered perfusion rate that leads to end-organ damage [22]. Percent myogenic tone is used to normalize vessel reactivity as it allows the comparison between vessels of varying thicknesses. Using pressure myography, the outer and inner diameter of an artery can be measured under different conditions. In order for myogenic tone to be measured, the artery must be pressurized in a buffer containing calcium and in a buffer without calcium. These buffers represent the active and passive conditions, respectively. Percent myogenic tone is calculated through the following equation [23]:

$$MT(\%) = \frac{ID_{passive} - ID_{active}}{ID_{passive}} \times 100\% \qquad (1)$$

where $ID_{Passive}$ is the internal diameter measured in the absence of calcium, and ID_{Active} is the internal diameter measured in the presence of calcium.

2.4 Arterial Stiffening

2.4.1 Arterial Stiffening and Cyclic Behavior

Arterial stiffening is the hardening of the arteries that results in decreased distensibility of the vessels [24]. A major property of blood vessels is the cyclic behavior of their components that aid in pushing the blood through the artery. However, living systems of the body are constrained by similar properties as nonliving systems. The cyclic property of arterial wall components is no exception and begins to break down, creating a major linkage between arterial stiffening and aging [25, 26]. The destruction of the elastic fibers in the wall of the artery leads to a stiffening of the vessel which, in turn, leads to a rise in aortic systolic blood pressure and a larger pulse that travels farther downstream through the arteries. The effect of arterial stiffening on vascular mechanics is illustrated in Figure 2. Other pathologies include hypertrophy of the left ventricle of the heart and decreased perfusion of blood out of the capillaries [27].

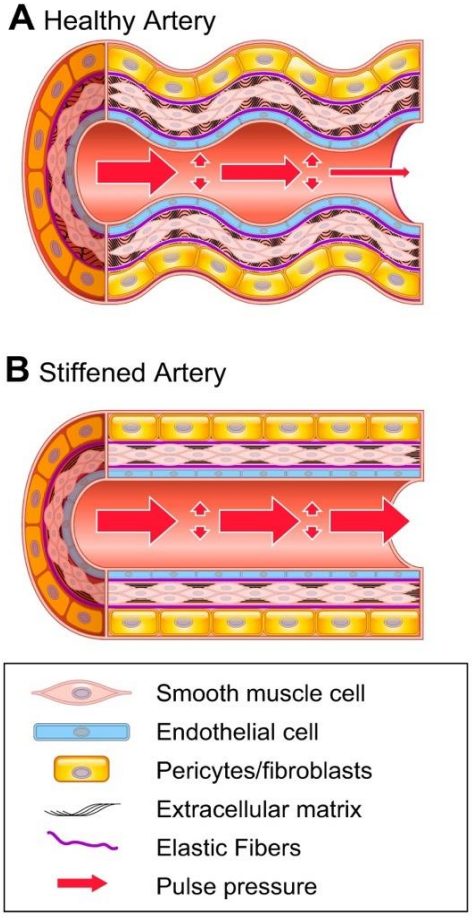

Figure 2. (A) The pulse pressure slowly decreases as it moves along a healthy vessel. (B) The pulse pressure does not decrease in stiffened arteries [29].

2.4.2 Pulse Wave Velocity

There are many techniques to measure arterial stiffness *in vivo*, but the most common and noninvasive method is pulse wave velocity [28]. Pulse wave velocity is measured using high-

frequency ultrasound between two points of an artery. In humans, the established locations are the bilateral brachial and ankle and carotid and femoral arteries [29]. Once the pulse wave is measured using the ultrasound, the distance between waveforms determines the time delay. Then, the distance between the two measured points is measured using either measuring tape [30] or an estimated equation [31]. Pulse wave velocity is calculated by dividing the distance between the two points by the waveform time delay. The technique explained above applies to measuring murine pulse wave velocity with an added benefit of measuring intracarotid length *in vivo*.

2.5 Vascular Endothelium and GPER

2.5.1 Endothelial Nitric Oxide Synthesis

The endothelium lines the inner circumference of the entire vascular system and plays a critical role in regulating vascular activity. The endothelium's role in vasodilation was first discovered in 1980 [32] and was later attributed to the production of nitric oxide (NO). Many factors are able to activate the pathway such as increased intracellular calcium concentrations, binding of acetylcholine [33], and shear stress [34]. In response to intracellular calcium, endothelial nitric oxide synthase activates and begins catalyzing L-Arginine to NO [35]. The synthesized NO then diffuses into the adjacent smooth muscle where it binds to guanylyl cyclase and increases cyclic guanosine monophosphate (cGMP) production. The cGMP then decreases muscle tension [36] and reduces smooth muscle contraction by reducing calcium release from the sarcoplasmic reticulum [37]. The pathway is illustrated in Figure 4.

2.5.2 Estrogen and Nitric Oxide

Estrogen plays an important role in regulating vascular tone by the production of NO [38, 39]. Specifically, GPER activates the NO synthesis pathway (Figure 4) when an agonist binds. Although the nuclear estrogen receptors are present in endothelial cells along with GPER, the vasodilation response is the same between exposure to 17β-estradiol and G-1 leading to GPER being the main contributor to vasodilation [5]. The interaction between the GPER and eNOS pathway can be seen in Figure 3.

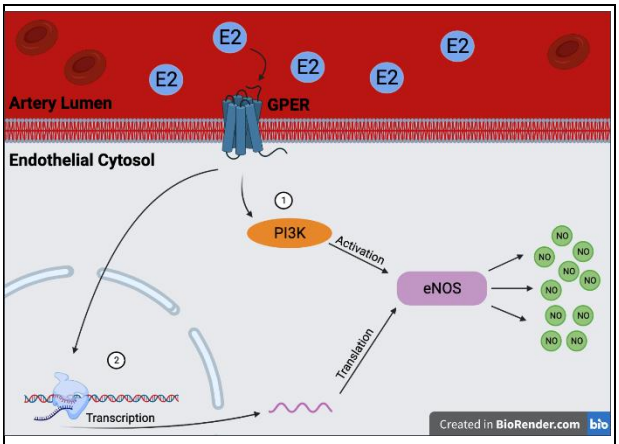

Figure 3. Interaction between eNOS and GPER.

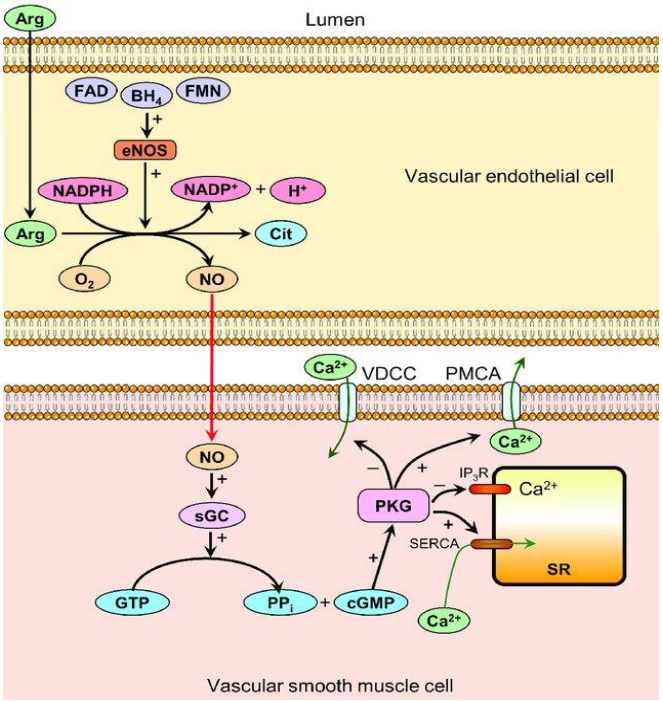

Figure 4. Pathway of nitric oxide synthesis vascular endothelial cells [40].

2.6 Objective

The goal of this study is to characterize myogenic tone in mice with endothelial dysfunction using active pressure myography as well as characterizing changes in wall thickness to determine extracellular matrix changes. Additionally, GPER's interaction with endothelial-derived vascular stiffening will be investigated. These experiments will be used as a basis for further investigation into the endothelium and GPER's role in cardiovascular disease.

We hypothesize that endothelial dysfunction induced by L-NAME treatment or GPER deletion will cause an increase in myogenic tone, vessel thickness, and pulse wave velocity without an increase in blood pressure.

3. Materials and Methods

3.1 Animal Care

All animal care and procedures were approved by the Tulane University Institutional Animal Care and Use Committee (IACUC). Male C57BL/6 mice were divided into four cohorts: wild-type (WT) control (n=4), WT treatment (n=3), G protein-coupled estrogen receptor (GPER) knockout (KO) control (n=4), and GPER KO treatment (n=3). Mice were provided with food and water *ad libitum* in a temperature-controlled room (18-25˚C) with a twelve-hour light to dark cycle. Treatment animals received N_{ω}-Nitro-L-arginine methyl ester hydrochloride (L-NAME, Sigma-Aldrich) in the drinking water (0.5 g/L) for three weeks as described in Fitch et al [40].

3.2 Blood Pressure

Blood pressure was measured via tail-cuff plethysmography using the CODA™ Noninvasive Blood Pressure System (Kent Scientific, Torrington, CT). Baseline blood pressures were measured the week before the initiation of treatment and throughout the three weeks of L-NAME treatment. Mice were restrained as shown in figure 1, and the tail was warmed to 35˚C ± 2˚C for the duration of blood pressure measurements via a warming platform. Readings were manually filtered for the return of blood flow after cuff deflation as indicated by a clear inflection point. Daily values were averaged using a MATLAB code in which values not ± 2 standard deviations from the mean were excluded.

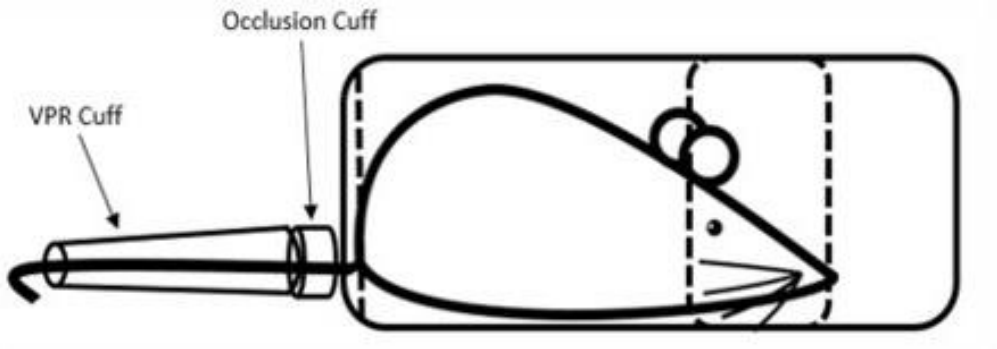

Figure 5. Courtesy of Isabella Kilanowski-Doroh

3.3 Pulse Wave Velocity

3.3.1 Carotid Pulse Wave Velocity

Pulse Wave Velocity (PWV) was measured using the Vevo® 1100 ultrasound (VisualSonics, Toronto, ON). Anesthesia was induced using 3% isoflurane/oxygen mixture and maintained at 1-2% isoflurane/oxygen by nose cone throughout the procedure. Once the EKG platform reached 37˚C, the mouse was placed in a supine position with its limbs securely fastened with surgical tape, and eye ointment was applied. Depilatory cream was applied to the throat, chest, and abdomen and removed after two minutes with a wet gauze. To measure PWV, the carotid was imaged in longitudinal view from the aortic arch to the carotid bifurcation as shown in Figure 6. Pulse wave arrival was measured using both wall movement in M-mode and arrival of flow in color doppler. Indications of peak arrival time was determined as the inflection point of wall movement in M-mode and peak velocity in color doppler. To determine transit time, arrival time was subtracted from the time of the R-wave. The ultrasound built-in ruler tool was used to measure the distance between the proximal and distal carotid points previously used for arrival time. PWV can be found using the following equation:

$$PWV_{Carotid} = \frac{d_{carotid}}{t_{diff}} \qquad (2)$$

where $d_{carotid}$ is the distance between the proximal and distal measured points, and t_{diff} is the difference in the proximal and distal transit time.

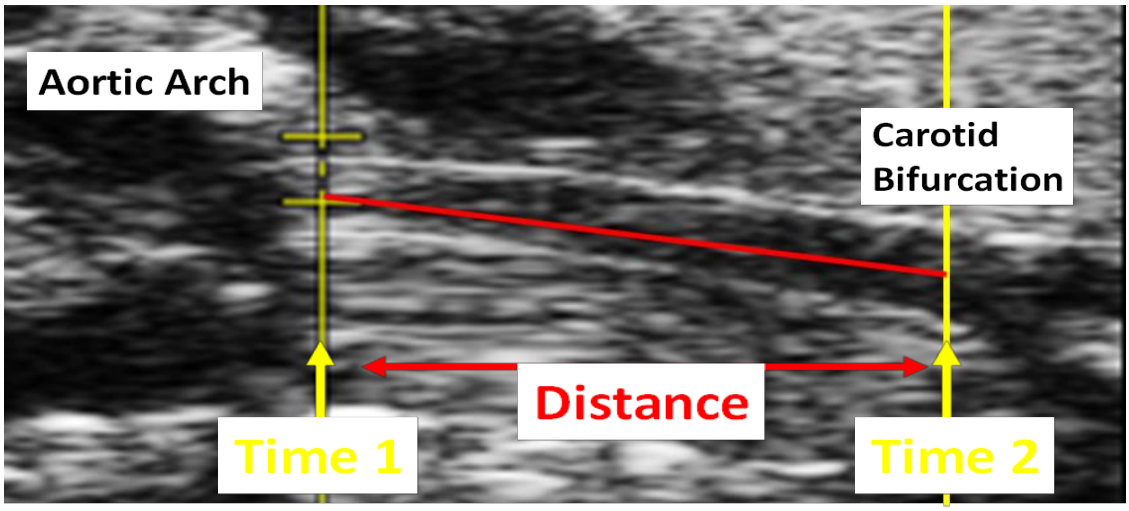

Figure 6. Visualization of carotid in longitudinal view.

3.4 Tissue Harvesting

Mice aged 22-25 weeks were euthanized under deep isoflurane followed by removal of the diaphragm and heart. A midsagittal laparotomy was performed by first removing the skin from the pelvis to the sternum. Then, the underlying muscle layer and the peritoneum were removed. Next, the proximal end of the intestines close to the pylorus and the distal end close to the ileo-cecal junction was cut. The entire intestinal bed, which includes the mesenteric artery arcade, was transferred to a conical tube containing ice-cold active buffer (118 mM NaCl, 4.8 mM KCl,1.2 $MgSO_4$, 25 mM $NaHCO_3$, 1.2 mM KH_2PO_4, 2.5 mM $CaCl_2$, 11.1 mM Dextrose, 10 µM EDTA) for at least five minutes to get rid of excess blood. Once the intestines were rinsed, 28g needles were used to pin down the intestinal bed onto a sylgard-coated dish from the proximal end of the intestine to the distal end in a counterclockwise fashion as shown in Figure 7.

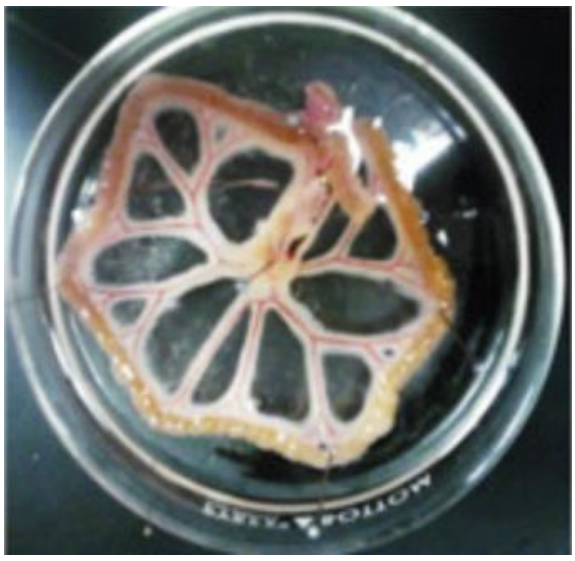

Figure 7. Intestines pinned in sylgard-coated dish [9].

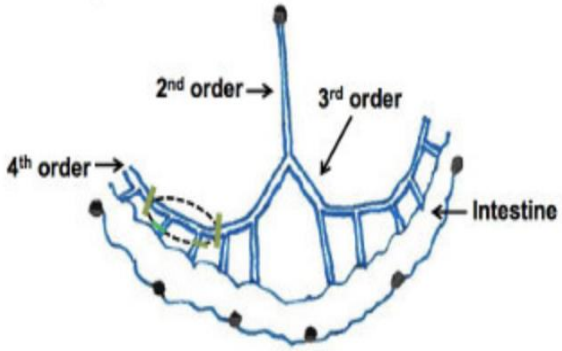

Figure 8. Diagram of the mesenteric arcade [9].

Once the blood vessels are exposed, a section of a 2nd order artery (Figure 8) was dissected away from the surrounding adipose and connective tissue and placed in cold, active buffer. The proximal end of the dissected artery was noted to ensure correct orientation during cannulation.

3.5 Mechanical Testing

3.5.1 Active Pressure Myography

The protocol for assessing myogenic tone using pressure myography of mesenteric arteries was adapted from *Jadeja et al* [9] and is included in the supplemental materials. The dissected 2nd order mesenteric artery was mounted onto 100-150 µm diameter glass cannulas using dissection forceps and tied down with 3-0 sutures. The stage was then connected to the pressure-myography system (MyoVIEW, Danish Myo Technology A/S, Aurhus N, Denmark) shown in Figure 9. The vessel was washed with fresh active buffer, and the temperature was slowly brought up to 37˚C. Oxygenation was maintained using a gas mixture of 5% CO_2 and 95% O_2. The vessel was stretched to passive, non-bulging length and washed with fresh buffer through the lumen. The vessel was then pressurized to 140 mmHg to test the integrity of the vessel and sutures. After initial testing,

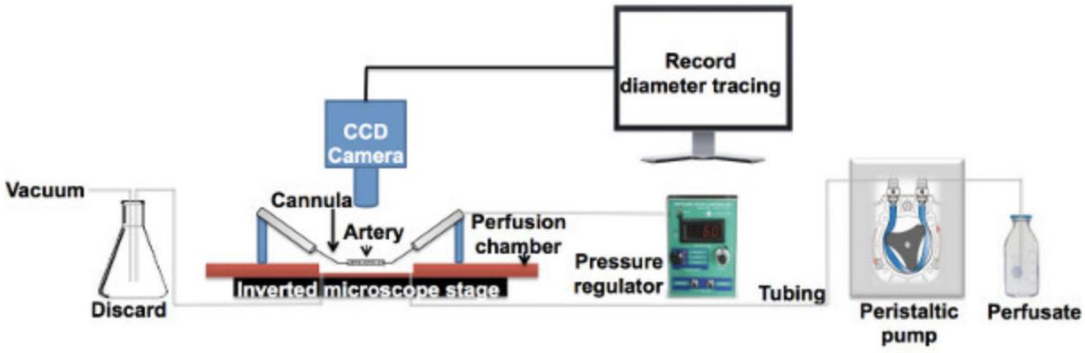

Figure 9. Setup of DMT system [9]

the vessel was equilibrated at 70 mmHg and 37˚C for 20 minutes. The outer and inner diameters of the vessels were optically tracked (Eclipse TS100 video-microscope, Nikon, Melville, NY, U.S.A.). Next, the vessel was preconditioned from 20 mmHg to 140 mmHg three times to ensure recapitulation of *in vivo* behavior. Viability of the vessel was tested by creating a bath of 80 mM KCl and letting the vessel stabilize for five minutes. Viable vessels were then washed with active buffer to return to normal diameter. Finally, active pressure diameter curves were recorded by changing the pressure from 20 mmHg to 140 mmHg with 20 mmHg steps lasting sixty seconds. The use of stepwise pressure instead of continuous pressure allows proper time for a myogenic response.

3.5.2 Passive Pressure Myography

After the active pressure diameter curves were recorded, the vessel was washed three times with 37˚C passive buffer (118 mM NaCl, 4.8 mM KCl,1.2 $MgSO_4$, 25 mM $NaHCO_3$, 1.2 mM KH_2PO_4, 11.1 mM Dextrose, 10 μM EDTA). The vessel was allowed to equilibrate in passive buffer for 20 minutes at 70 mmHg. After equilibration, fresh passive buffer was added and brought to 37˚C. Three pressure diameter curves were recorded from 20 mmHg to 140 mmHg. To maintain consistency between the active and passive protocols, 20 mmHg stepwise pressure increases were used instead of continuous increases.

3.6 Data Analysis

Once the active and passive pressure diameter data were recorded, the raw data was transferred from the MyoView (MyoVIEW, Danish Myo Technology A/S, Aarhus N, Denmark) software to Microsoft Excel (Microsoft Excel, Microsoft Corportaion, Redmond, WA, U.S.A.). In order to bin the large number of diameters at each pressure, a MATLAB code was created and used to average the diameters in intervals of 20 mmHg ± 2 mmHg. Once the outer and inner diameters were averaged, myogenic tone was calculated using the following equation [23]:

$$MT(\%) = \frac{ID_{passive} - ID_{active}}{ID_{passive}} \times 100\% \qquad (3)$$

where $ID_{Passive}$ is the passive inner diameter and ID_{Active} is the active inner diameter. Vessel wall thickness was calculated using the following equation at each pressure:

$$Thickness(\mu m) = \frac{OD_p - ID_p}{2} \qquad (4)$$

where OD_P is the passive outer diameter, and ID_P is the passive inner diameter.

3.7 Statistical Analysis

Student's t-test was used to assess the change in PWV, and one-way analysis of variance (ANOVA) was used to assess changes in blood pressure to validate the efficacy of the L-NAME treatment. Two-way ANOVA was used to analyze vessel inner and outer diameter, thickness, and reactivity between L-NAME treatment and genotype. Tukey's Test was used for posthoc analysis. A p value < 0.05 was considered significant, and all presented data is mean ± SEM.

4. Results

4.1 Blood Pressure and Pulse Wave Velocity

There was a significant difference between baseline PWV pre- and post-L-NAME treatment as shown in Figure 10. There was no difference between the PWV increase between GPER(WT) and GPER(KO) mice (Figure 11). Additionally, there was no significant change in blood pressure during the experiment in any of the four cohorts (Figure 12).

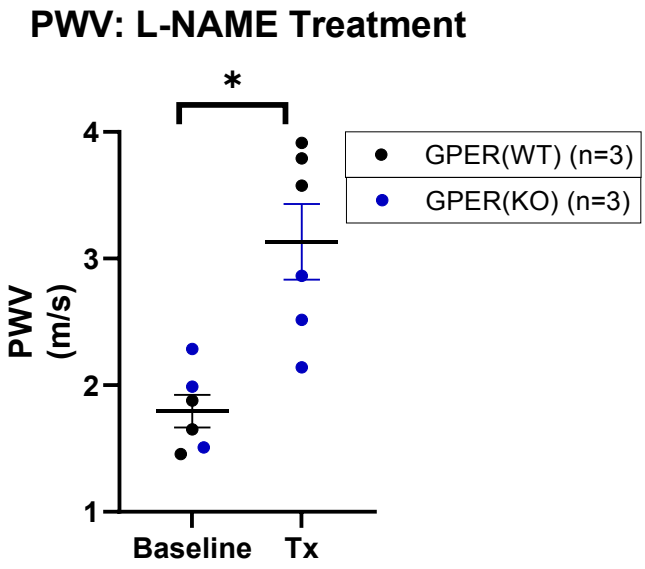

Figure 10. There was a significant difference between baseline and post-L-NAME treatment PWV in both GPER wild-type and knockout groups.
**Paired t-test, P = 0.0122*

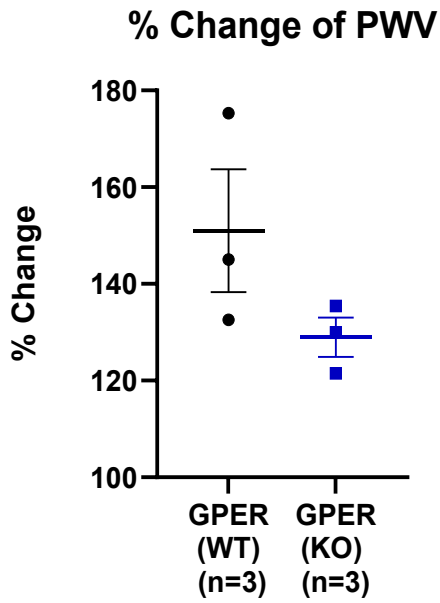

Figure 11. There was no significant difference in the % change of PWV between GPER(WT) and GPER(KO) animals.
Unpaired t-test P>0.05

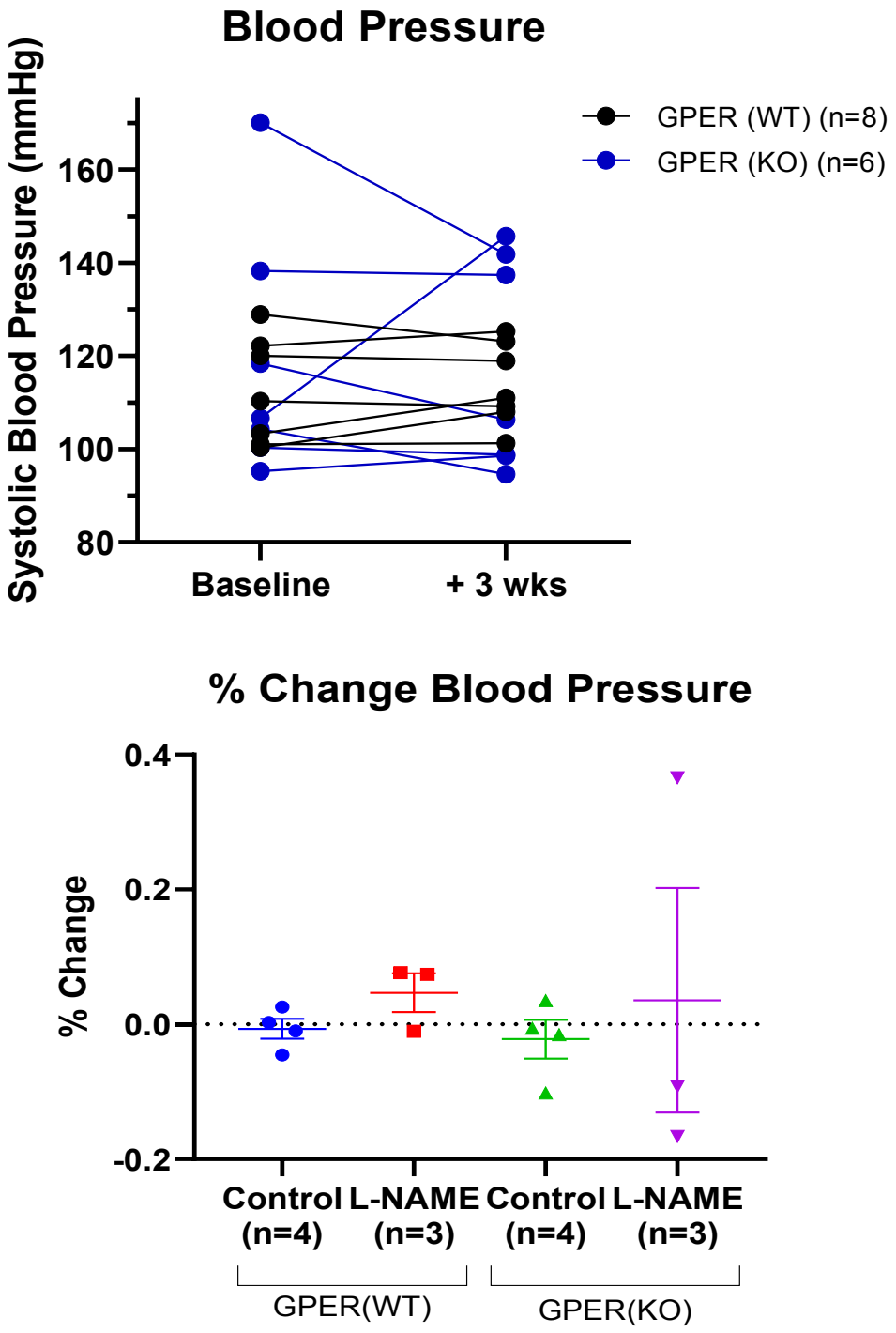

Figure 12 a-b. No change in blood pressure after L-NAME treatment.

Ordinary one-way ANOVA, P>0.05

4.2 Thickness

Second order mesenteric artery wall thickness was optically recorded during passive pressure myography. There was no significant difference in mesenteric wall thickness at 20 mmHg between all four of the groups as shown in Figure 13.

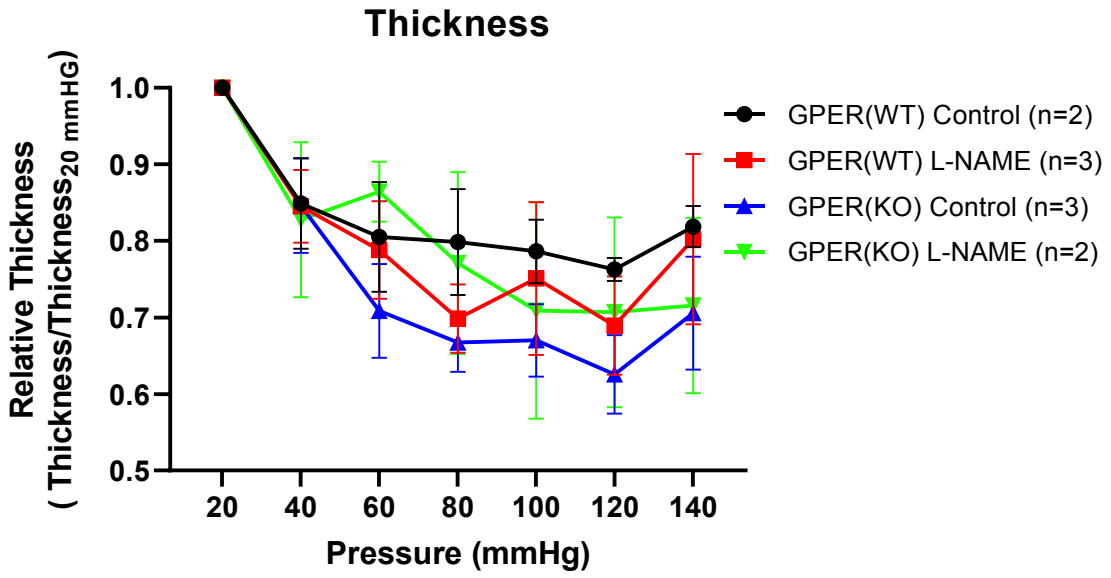

Figure 13. No significant difference in mesenteric wall thickness existed between the four groups. P>0.05, Two-way ANOVA.

4.3 Myogenic Tone

Active pressure myography was performed as described above and calculated using Equation 3. GPER KO mice exhibited a higher degree of myogenic tone when compared to their WT counterparts. Chronic treatment of L-NAME in WT mice significantly increased the myogenic contraction of the mesenteric artery when compared to control mice. Inversely, L-NAME treatment significantly decreased the myogenic tone in KO mice. Percent myogenic tone is shown in Figure 14. Normalized active and passive inner and outer diameter for each group is shown in Figure 15a-d for comparison.

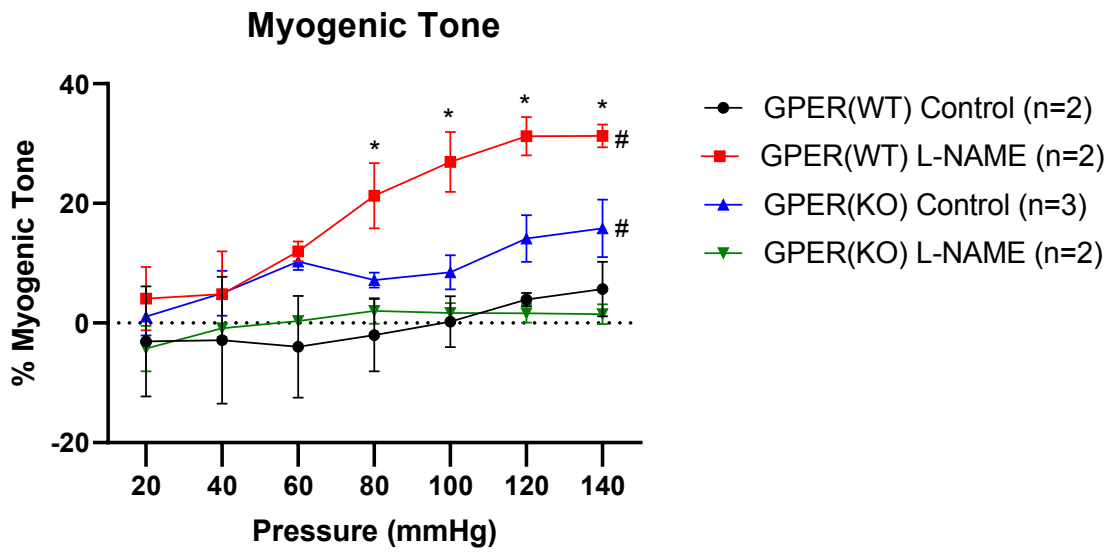

Figure 14. Percent myogenic tone.

**p<0.05 Two-way ANOVA; Pressure-dependent*

#p<0.05 Two-way ANOVA; Pressure-independent

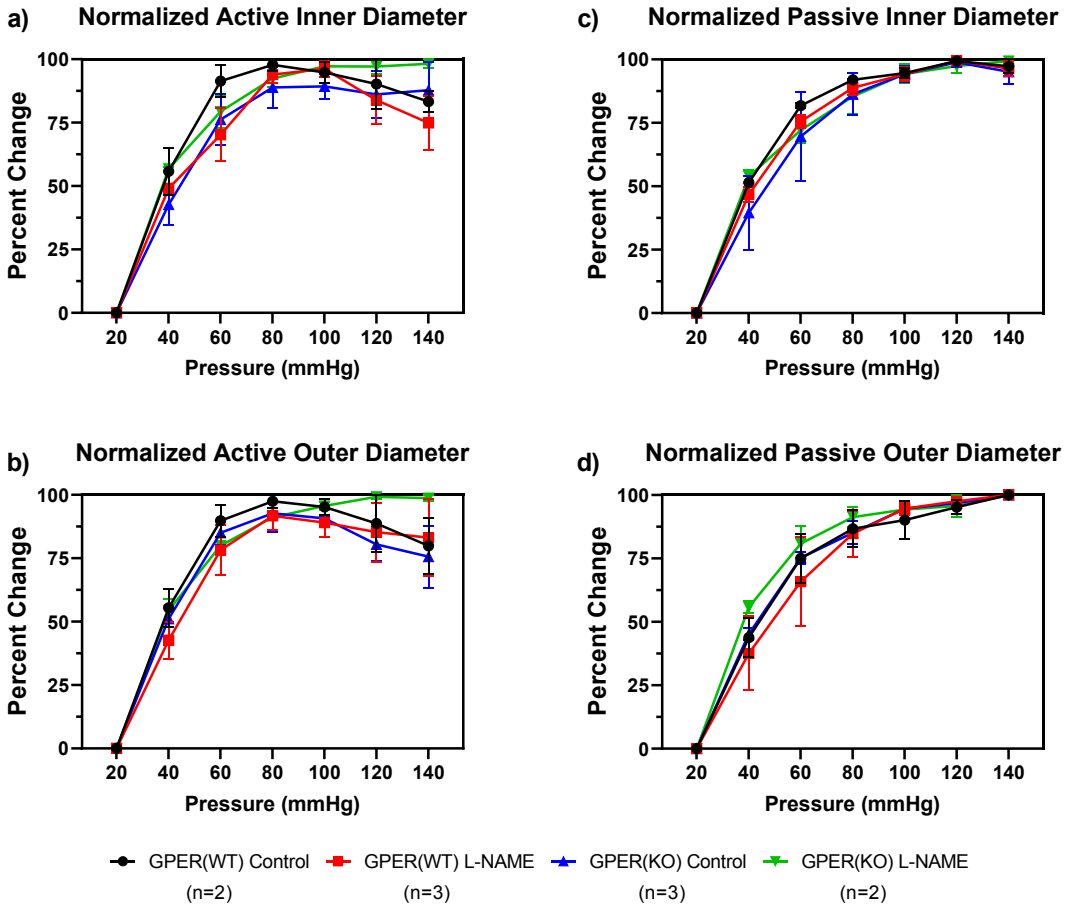

Figure 15 a-d. No significant difference between normalized inner or outer diameter in passive or active conditions. P>0.05, Two-way ANOVA

5. Discussion

Endothelial dysfunction is an important part of cardiovascular disease. Unfortunately, the pathology of the endothelium in small resistance arteries is understudied; leaving a gap in our understanding of the pathophysiology of cardiovascular disease. In this study, mesenteric arteries from GPER wild-type mice that received chronic L-NAME treatment showed an increase in myogenic tone when compared to GPER wild-type mice that did not receive L-NAME treatment (Figure 14). The increased myogenic tone is due to the inhibited production of the vasodilatory signal NO. Without NO signaling, high pressure caused the vascular smooth muscle cells to constrict more than physiologically normal. A previous study found that acute treatment of L-NAME to vessels with increased basal NO production abolished the inhibition of myogenic tone. This study highlights the regulation of myogenic tone includes both myogenic contraction and NO signaling [41]. L-NAME treated WT mice also experienced an elevation in PWV (Figure 10), signifying stiffening of the artery, but did not have an increase in blood pressure or vascular thickness (Figures 12 and 13). Stiffening of large arteries is frequently associated with aging and endothelial dysfunction [42]. Increased stiffness is associated with extracellular matrix remodeling and deposition of collagen which leads to a thicker arterial wall. In this study, increased carotid stiffness was not associated with increased arterial wall thickness in small resistance arteries such as the mesenteric artery; signifying increased stiffening does not necessarily cause remodeling of small resistance arteries. This concept can be further seen in Figure 15 as there is no difference in passive normalized curves between the groups. Deviation is seen in the active conditions; two hypotheses can be drawn from this. First, the vascular smooth muscle cells themselves are becoming stiffer or their ECM fibers are crosslinking. Furthermore, the endothelial cells or vascular smooth muscle cells, themselves, are at the root of the change due to biochemical changes making them more vasodilatory or vasoconstrictive. Further research is needed to determine the biochemical and extracellular matrix composition changes that occur with stiffening of small resistance arteries such as the mesenteric artery.

GPER KO mice had increased myogenic tone when compared to their WT counterparts, indicating GPER's involvement in vasodilation. These results are consistent with a previous study that showed GPER-mediated vasodilation involves the production of NO in the endothelium and cyclic adenosine monophosphate in vascular smooth muscle [39]. Contrary to the results in WT mice, L-NAME treatment in KO did not amplified myogenic tone. Thus, myogenic tone in GPER WT mice that did not receive L-NAME was not significantly different from that of L-NAME treated KO mice. These results show a divergence in the effects of L-NAME when estrogen-dependent endothelial signaling was not present.

The results of the L-NAME treatment in GPER KO mice were unexpected. With the inhibition of NO production and the loss of the GPER pathway, it was expected these animals would show greater arterial stiffness and myogenic tone than their GPER KO control counterparts and the L-NAME treated WT mice. However, these mice did exhibit arterial stiffening in response to L-NAME treatment, and myogenic tone was similar to that of WT control mice. One explanation for the smaller myogenic tone when compared to GPER KO control mice is the toxic effects produced by excess NO production. In order to counteract the loss of the vasodilation by estrogen, the cell may produce more NO. Excess NO can react with superoxide to form peroxynitrite (ONOO-) which oxidizes cellular components resulting in cytotoxicity [43]. Previous studies have also shown that reactive oxygen species like NO, superoxide, and peroxynitrite can cause the release of NO from the guanidino nitro group of L-NAME [44]. This NO release would essentially attenuate the inhibitory effect of NO production on the L-NAME treated mice. Alternatively, the global knockout of GPER like the model used in this study may affect other systems in the body that could influence myogenic tone. For example, many cells in the immune system present in the cardiovascular system such as resident macrophages are known to have GPER present that plays a role in immunoregulation [45]. These theories may explain the reduced degree of arterial stiffening in GPER KO mice. Further, peroxynitrite assays and studies

involving an inducible eNOS knockout model would elucidate these unexpected results in this study.

In conclusion, this study provides evidence of the complicated roles of GPER and NO in endothelial cell-mediated vasodilation. While the first hypothesis that NO inhibition would increase arterial stiffening and myogenic tone was supported, the exact role of estrogen in the development of cardiovascular disease is still unclear. Further testing that includes larger sample sizes, histological testing for extracellular matrix components, and biochemical assays for cellular compliance will provide a clearer picture of the endothelium's role in small resistance vessel pathology. Understanding estrogen's effect on endothelial dysfunction could reveal important therapeutic targets.

References

1. Heron, M., *Deaths: Leading causes for 2016.* National Vital Statistics Reports, 2018. **67**(6).
2. Kaess, B.M., et al., *Aortic Stiffness, Blood Pressure Progression, and Incident Hypertension.* JAMA, 2012. **308**(9): p. 875-881.
3. Åstrand, H., et al., *In vivo estimation of the contribution of elastin and collagen to the mechanical properties in the human abdominal aorta: effect of age and sex.* Journal of Applied Physiology, 2011. **110**(1): p. 176-187.
4. Tomiyama, H., *Arterial Stiffness: Is This a Marker for the Current Status or Future?* Journal of atherosclerosis and thrombosis, 2016. **23**(9): p. 1026-1027.
5. Lindsey, S.H., et al., *Vasodilation in response to the GPR30 agonist G-1 is not different from estradiol in the mRen2.Lewis female rat.* Journal of cardiovascular pharmacology, 2011. **57**(5): p. 598-603.
6. Fredette, N.C., M.R. Meyer, and E.R. Prossnitz, *Role of GPER in estrogen-dependent nitric oxide formation and vasodilation.* The Journal of steroid biochemistry and molecular biology, 2018. **176**: p. 65-72.
7. Pistner, A., et al., *Murine Echocardiography and Ultrasound Imaging.* JoVE, 2010(42): p. e2100.
8. Wang, Y., S.E. Thatcher, and L.A. Cassis, *Measuring Blood Pressure Using a Noninvasive Tail Cuff Method in Mice*, in *The Renin-Angiotensin-Aldosterone System: Methods and Protocols*, S.E. Thatcher, Editor. 2017, Springer New York: New York, NY. p. 69-73.
9. Jadeja, R.N., et al., *Assessing Myogenic Response and Vasoactivity In Resistance Mesenteric Arteries Using Pressure Myography.* Journal of visualized experiments : JoVE, 2015(101): p. e50997-e50997.
10. Mosca, L., E. Barrett-Connor, and N.K. Wenger, *Sex/gender differences in cardiovascular disease prevention: what a difference a decade makes.* Circulation, 2011. **124**(19): p. 2145-2154.
11. Lerner, D.J. and W.B. Kannel, *Patterns of coronary heart disease morbidity and mortality in the sexes: a 26-year follow-up of the Framingham population.* American heart journal, 1986. **111**(2): p. 383-390.
12. Iorga, A., et al., *The protective role of estrogen and estrogen receptors in cardiovascular disease and the controversial use of estrogen therapy.* Biology of sex differences, 2017. **8**(1): p. 33-33.
13. Manson, J.E., et al., *Estrogen therapy and coronary-artery calcification.* N Engl J Med, 2007. **356**(25): p. 2591-602.
14. Yang, X.-P. and J.F. Reckelhoff, *Estrogen, hormonal replacement therapy and cardiovascular disease.* Current opinion in nephrology and hypertension, 2011. **20**(2): p. 133-138.
15. Levin, E.R., *Cell localization, physiology, and nongenomic actions of estrogen receptors.* J Appl Physiol (1985), 2001. **91**(4): p. 1860-7.
16. Olde, B. and L.M. Leeb-Lundberg, *GPR30/GPER1: searching for a role in estrogen physiology.* Trends Endocrinol Metab, 2009. **20**(8): p. 409-16.
17. Revankar, C.M., et al., *A Transmembrane Intracellular Estrogen Receptor Mediates Rapid Cell Signaling.* Science, 2005. **307**(5715): p. 1625-1630.

18. Aronica, S.M., W.L. Kraus, and B.S. Katzenellenbogen, *Estrogen action via the cAMP signaling pathway: stimulation of adenylate cyclase and cAMP-regulated gene transcription.* Proc Natl Acad Sci U S A, 1994. **91**(18): p. 8517-21.
19. Improta-Brears, T., et al., *Estrogen-induced activation of mitogen-activated protein kinase requires mobilization of intracellular calcium.* Proc Natl Acad Sci U S A, 1999. **96**(8): p. 4686-91.
20. Filardo, E.J., et al., *Estrogen-induced activation of Erk-1 and Erk-2 requires the G protein-coupled receptor homolog, GPR30, and occurs via trans-activation of the epidermal growth factor receptor through release of HB-EGF.* Mol Endocrinol, 2000. **14**(10): p. 1649-60.
21. Avolio, A., *Arterial Stiffness.* Pulse (Basel, Switzerland), 2013. **1**(1): p. 14-28.
22. Sweazea, K.L. and B.R. Walker, *Impaired myogenic tone in mesenteric arteries from overweight rats.* Nutrition & metabolism, 2012. **9**(1): p. 18-18.
23. Wang, S., et al., *Sex differences in the structure and function of rat middle cerebral arteries.* American Journal of Physiology-Heart and Circulatory Physiology, 2020. **318**(5): p. H1219-H1232.
24. Avolio, A. and A. Avolio, *Arterial Stiffness.* Pulse, 2013. **1**(1): p. 14-28.
25. Rigby, B., *Effect of cyclic extension on the physical properties of tendon collagen and its possible relation to biological ageing of collagen.* Nature, 1964. **202**(4937): p. 1072-1074.
26. Fonck, E., et al., *Effect of Aging on Elastin Functionality in Human Cerebral Arteries.* Stroke, 2009. **40**(7): p. 2552-2556.
27. O'Rourke, M.F. and J. Hashimoto, *Mechanical Factors in Arterial Aging: A Clinical Perspective.* Journal of the American College of Cardiology, 2007. **50**(1): p. 1-13.
28. Blacher, J., et al., *Aortic Pulse Wave Velocity as a Marker of Cardiovascular Risk in Hypertensive Patients.* Hypertension, 1999. **33**(5): p. 1111-1117.
29. Tanaka, H., et al., *Comparison between carotid-femoral and brachial-ankle pulse wave velocity as measures of arterial stiffness.* Journal of Hypertension, 2009. **27**(10).
30. Tanaka, H., C.A. DeSouza, and D.R. Seals, *Absence of Age-Related Increase in Central Arterial Stiffness in Physically Active Women.* Arteriosclerosis, Thrombosis, and Vascular Biology, 1998. **18**(1): p. 127-132.
31. Sugawara, J., et al., *Agreement between carotid and radial augmentation index: Does medication status affect the relation?* Artery Research, 2008. **2**(2): p. 74-76.
32. Furchgott, R.F. and J.V. Zawadzki, *The obligatory role of endothelial cells in the relaxation of arterial smooth muscle by acetylcholine.* Nature, 1980. **288**(5789): p. 373-376.
33. Moncada, S. and E.A. Higgs, *The discovery of nitric oxide and its role in vascular biology.* British journal of pharmacology, 2006. **147 Suppl 1**(Suppl 1): p. S193-S201.
34. Kuchan, M.J. and J.A. Frangos, *Role of calcium and calmodulin in flow-induced nitric oxide production in endothelial cells.* American Journal of Physiology-Cell Physiology, 1994. **266**(3): p. C628-C636.
35. Palmer, R.M.J., D.S. Ashton, and S. Moncada, *Vascular endothelial cells synthesize nitric oxide from L-arginine.* Nature, 1988. **333**(6174): p. 664-666.

36. Jones, K.A., et al., *cGMP modulation of Ca2+ sensitivity in airway smooth muscle.* American Journal of Physiology-Lung Cellular and Molecular Physiology, 1999. **276**(1): p. L35-L40.
37. Collins, P., et al., *Endothelium-derived relaxing factor alters calcium fluxes in rabbit aorta: a cyclic guanosine monophosphate-mediated effect.* The Journal of physiology, 1986. **381**(1): p. 427-437.
38. Arnal, J.-F., et al., *Estrogen Receptors and Endothelium.* Arteriosclerosis, Thrombosis, and Vascular Biology, 2010. **30**(8): p. 1506-1512.
39. Lindsey, S.H., L. Liu, and M.C. Chappell, *Vasodilation by GPER in mesenteric arteries involves both endothelial nitric oxide and smooth muscle cAMP signaling.* Steroids, 2014. **81**: p. 99-102.
40. Fitch, R.M., et al., *Nitric oxide synthase inhibition increases aortic stiffness measured by pulse wave velocity in rats.* Cardiovascular Research, 2001. **51**(2): p. 351-358.
41. Skarsgard, P.L., et al., *Profound Inhibition of Myogenic Tone in Rat Cardiac Allografts Is Due to eNOS- and iNOS-Based Nitric Oxide and an Intrinsic Defect in Vascular Smooth Muscle Contraction.* Circulation, 2000. **101**(11): p. 1303-1310.
42. Shirwany, N.A. and M.-h. Zou, *Arterial stiffness: a brief review.* Acta pharmacologica Sinica, 2010. **31**(10): p. 1267-1276.
43. Beckman, J.S. and W.H. Koppenol, *Nitric oxide, superoxide, and peroxynitrite: the good, the bad, and ugly.* Am J Physiol, 1996. **271**(5 Pt 1): p. C1424-37.
44. Liu, T., et al., *L-NAME releases nitric oxide and potentiates subsequent nitroglycerin-mediated vasodilation.* Redox biology, 2019. **26**: p. 101238-101238.
45. Notas, G., M. Kampa, and E. Castanas, *G Protein-Coupled Estrogen Receptor in Immune Cells and Its Role in Immune-Related Diseases.* Frontiers in Endocrinology, 2020. **11**(774).

S1. Supplemental Materials and Methods

Glass Cannulas

1. Load a glass capillary into the SU-P1000 Micropipette Puller. Create the glass cannulas using these settings:
   Heat: 561
   Pull: 0
   Velocity: 120
   Time: 200
   Pressure: 200
   Ramp: 531

Solutions

Active Buffer:

Component	Concentration
NaCl	118 mM
KCl	4.8 mM
$MgSO_4$	1.2 mM
$NaHCO_3$	25 mM
KH_2PO_4	1.2 mM
$CaCl_2$	2.5 mM
Dextrose	11.1 mM
EDTA	10 µM

Passive Buffer:

Component	Concentration
NaCl	118 mM
KCl	4.8 mM
$MgSO_4$	1.2 mM
$NaHCO_3$	25 mM
KH_2PO_4	1.2 mM
Dextrose	11.1 mM
EDTA	10 µM

****Bubble buffers with 95% O2, 5% CO2 for 10-15 minutes****

Prepare the chamber

1. Flush all the lines with active myography buffer to ensure no air bubbles are present in the tubing.

Tissue Collection

2. Euthanize animal using Isoflurane.
3. Open the abdominal cavity and dissect out the mesenteric tissue by cutting the duodenum after the pyloric sphincter and at the sigmoid colon-rectum border.

4. Allow harvested tissue to stay in ice cold active buffer for 5 minutes.
5. Transfer tissue to a sylgard-coated dish.
6. Extend the remaining intestine in a counterclockwise path proximally to distally, pinning the segment down using 28g needles to spread the mesentery and expose the blood vessels.
7. Isolate and dissect a mesenteric artery of 2nd order free of connective and adipose tissue.
8. Place the artery in ice-cold active buffer solution.
9. Be sure to mark/note the portion of the cut artery proximal to the aorta.

Cannulate Specimen

10. Place the heated, active buffer-filled bath under the dissection microscope.
11. Place two double knotted nylon sutures loosely over the shaft of each glass pipette and transfer the isolated artery to the chamber of the pressure myograph.
12. Use two tweezers to hold the proximal end of the artery and slip it over the P1 cannula.
13. Tie off P1 and slip the distal end of the artery over P2. Tie off P2.
14. Install the chamber on the myograph under the video camera. Bubble the chamber with 95% O_2, 5% CO_2 gas and heat the chamber to 37 °C.

Pressure Myography Setup and Preconditioning

15. Go to the pressure menu on the myo-interface panel or in the DMT software and turn **ON**.
16. Stretch the arterial segment longitudinally to passive, non-bulging length.
17. Wash with 5 mL fresh active buffer.
18. Flow (P1: 70 mmHg; P2: 10 mmHg) for 5 minutes.
19. Test suture integrity by increasing pressure to 140 mmHg for 2 minutes.
20. Wash with fresh active buffer.
21. Equilibrate the vessel at **70 mmHg and 37 °C at least for 20 min**.
22. Open tabs for OD, ID, Force, and Inlet Pressure and **Press START.**
23. Increase pressure from 20 mmHg to 140 mmHg three times to precondition.
    a. Watch the force - it should be stable indicating it's at the right length.
24. Test viability by adding 80mM KCl (3M stock solution= add 0.133ml to 5ml bath) and let the vessel stabilize for 5 minutes.
25. Wash 3 times with active buffer every 5 minutes.
    a. Continue washes if outer diameter continues to increase.

Active- Vascular Reactivity

1. Record 3x Pressure diameter curve 20mmHg-140mmHg at 20 mmHg steps.
    a. Allow 30 seconds at each step to allow time for vessel to react.

Passive- Stiffness and Remodeling

1. Wash the vessel 3x5 minutes with passive buffer.
2. Equilibrate in Ca^{2+} free buffer for **20-30 min at 37 °C and 70 mmHg.**
3. Add fresh passive buffer and allow temperature to reach **37 °C**.

4. Record 3x pressure diameter curves 20mmHg-140mmHg.
    a. 30 seconds step duration to mimic active protocol.
    b. If the vessel is still contracting, perform 3 washes with passive buffer.

Clean-up

1. Remove and dispose of vessel properly.
2. Clean p-myo chamber and tubing by diluting one drop of 1N HCl in 5mL Milli-Q H_2O.
3. Flow clean Milli-Q H_2O through p-myo machine and chamber.
4. Allow air to flow for 15 minutes to dry the entire system.